Cold-end corrosion caused by hygroscopic ammonium chloride in thermal conversion of biomass and waste

Vainio, Emil; Yrjas, Patrik; Hupa, Leena; Hupa, Mikko

Published in:
Fuel

DOI:
10.1016/j.fuel.2023.128061

Published: 15/08/2023

Document Version
Final published version

Document License
CC BY

Fuel 346 (2023) 128061

Contents lists available at ScienceDirect

Fuel

journal homepage: www.elsevier.com/locate/fuel

Cold-end corrosion caused by hygroscopic ammonium chloride in thermal conversion of biomass and waste

Emil Vainio *, Patrik Yrjas, Leena Hupa, Mikko Hupa

Johan Gadolin Process Chemistry Centre, Combustion and Materials Chemistry Group, Åbo Akademi University, Turku, Finland

ARTICLE INFO

Keywords:
Cold-end corrosion
NH_4Cl
Hygroscopic
Deliquescent
Carbon steel

ABSTRACT

Optimization of energy recovery and efficient use of the energy in flue gases is of high importance for the economy of power plants. The fuel quality and additives to mitigate corrosion may dramatically affect cold-end deposits and corrosion. Ammonium chloride may form in the cold-end of the boiler if the flue gases contain both HCl(g) and NH_3(g). Ammonia may be present in the cold-end when using ammonium-based additives or operating the boiler at low load leading to an NH_3(g) slip. Ammonium chloride is a hygroscopic salt, which can cause corrosion of pre-heaters and flue gas cleaning equipment NH_3(g) and HCl(g) can also pass through filters and form NH_4Cl(s) after the baghouse filters. In this work, the hygroscopic properties of NH_4Cl were determined by measuring the conductivity of the salt during decrease of temperature at various water vapor concentrations (10–35 vol%). The corrosiveness of NH_4Cl salt on carbon steel was studied at 25 vol% water vapor in the temperature range of 70–160 °C. The cross-sections were analyzed using SEM-EDX, and corrosion rates were determined from panorama SEM images by analyzing the material loss in about 50 000 points. The material loss was also determined gravimetrically after removing the corrosion products with citric acid. The work revealed that hygroscopic NH_4Cl is highly corrosive on carbon steel when water is absorbed. Water uptake and corrosion occurred at relative humidities well below the deliquescence relative humidity and depended on the temperature. An empirical equation for water uptake by NH_4Cl was determined for water vapor concentrations between 10 and 35 vol% H_2O. As corrosion proceeded, chlorine was enriched close to the carbon steel surface due to the formation of iron chlorides. The results can be used to avoid conditions typical for NH_4Cl deposit build-up and create strategies to prevent corrosion.

1. Introduction

Cold-end corrosion and deposit build-up on cold-end heat transfer tubes and flue gas cleaning equipment are known issues. However, the reasons for these phenomena are not always understood. Generally, corrosion in the cold-end of power plants can be caused by dew point corrosion and hygroscopic deposits. When utilizing biomass and waste-derived fuels, the main causes of these problems are typically hygroscopic salts and deposits. These can cause corrosion of heat exchangers (air preheaters and economizers), flue gas duct walls, and flue gas cleaning equipment [1–7]. Hygroscopic salts can also lead to deposit build-up by forming wet and sticky deposits leading to a decrease in heat transfer and plugging of flue gas equipment, e.g., by forming dense filter cakes in baghouse filters [3,8]. Hygroscopic deposits may also initiate and cause corrosion during the shut-down of a boiler [9,10].

Several salts that are formed during thermal conversion of biomass and waste are hygroscopic and may, at a given temperature and humidity, even absorb enough water to fully dissolve in the water. This phenomenon is called deliquescence and may additionally influence deposits' tendency to cause corrosion. This critical humidity is called the deliquescence relative humidity or DRH. Deliquescent salts may cause corrosion at surface/deposit temperatures well above 100 °C [5]. The formation of deliquescent salts and deposits in energy conversion is influenced by the ash composition of the fuel, additives used (e.g., ammonia, limestone, lime), conversion technology, boiler operation, and flue gas composition. Ammonium chloride is a hygroscopic salt that has been reported to form and cause corrosion in the cold-end of boilers [11–14] and in oil refining units [15–18]. Hygroscopicity of NH_4Cl has

* Corresponding author.
E-mail address: emil.vainio@abo.fi (E. Vainio).

https://doi.org/10.1016/j.fuel.2023.128061
Received 15 December 2022; Received in revised form 25 February 2023; Accepted 3 March 2023
Available online 25 April 2023

been studied for atmospheric aerosols [19–21], storage and handling of fertilizers [22], and in atmospheric corrosion [23]. The DRH of NH_4Cl at room temperature is 77–79% [21,22]; however, the DRH has not been determined at flue gas conditions. Furthermore, NH_4Cl is also corrosive on carbon steel well below the DRH, by interacting with water vapor forming a corrosive environment [18,24]. Salts may adsorb water leading to corrosion at a relative humidity (RH) well below the DRH [25]. Dry ammonium chloride can also cause corrosion at higher temperatures. Herzog et al. [3] reported economizer corrosion in the range of 145–165 °C in a waste-fired boiler using selective non-catalytic reduction (SNCR) of NO_X emission, where pitting of the leeward side of the tubes occurred and $(NH_4)_2FeCl_5$ was identified as the corrosion product.

If the flue gases contain NH_3(g) and HCl(g), ammonium chloride may form on surfaces according to Reaction (1). The temperature at which NH_4Cl(s) forms depends on the NH_3(g) and HCl(g) concentrations. Fig. 1 shows the thermodynamic stability of NH_4Cl(s) at various NH_3(g) and HCl(g) concentrations. NH_4Cl(s) forms at conditions representing the left side of the lines. At conditions on the right side of the lines, NH_4Cl(s) dissociates to NH_3(g) and HCl(g) [26].

$$NH_3(g) + HCl(g) \leftrightarrow NH_4Cl(s) \quad (1)$$

Ammonium-based additives for NO_X reduction will lead to an NH_3(g) slip [6]. If HCl(g) is present in the flue gases, it can lead to the formation of NH_4Cl(s). It has even been shown during low-load operation of a circulating fluidized bed boiler that NH_3(g) formed from the fuel nitrogen formed NH_4Cl(s) in the presence of HCl(g) in the cold-end [11]. The ammonia survived in this case due to low furnace temperatures caused by the low load of the boiler (55%) [11]. Fig. 2 depicts the formation routes of NH_4Cl(s) from fuel nitrogen, ammonium-based additives, and HCl(g). Since NH_4Cl(s) forms from gaseous NH_3 and HCl, it can also form downstream after the baghouse filters.

The hygroscopicity and corrosivity of NH_4Cl in flue gas conditions are not fully understood. In this work, the hygroscopic properties of NH_4Cl were studied to determine the conditions at which the salt can cause corrosion on carbon steel. The hygroscopic properties of NH_4Cl were studied by measuring the conductivity of the salt during decreasing of the temperature at various water vapor concentrations (10–35 vol%). Furthermore, the corrosivity of NH_4Cl on carbon steel in the temperature range of 70–160 °C and 25 vol% H_2O was assessed.

2. Experimental

2.1. Measurement of hygroscopic properties of NH_4Cl

The hygroscopic properties of NH_4Cl were measured through the conductivity of the salt measured at various water vapor concentrations (10–35 vol%). Two-electrode chronoamperometry (CA) was used to detect water uptake by the salt. The current was measured using an EmStat4s portable potentiostat. One of the electrodes was employed as the working electrode, and the other as the counter/reference electrode. The NH_4Cl salt was dried overnight at 105 °C and placed in a crucible made of silica. Titanium electrodes were placed in the salt, and the voltage between the electrodes was set to 1000 mV. The electrodes were Teflon-coated, apart from the measuring tips, to avoid any signal disturbance from water condensation at the cold-end of the tube furnace used in the experiments. The crucible with the salt was placed in a tube furnace with a flow of N_2 gas at approximately 120 °C. When the salt had reached the furnace temperature, water vapor was added to the gas. The steam was produced with a Cellkraft P-2 steam generator. The temperature was slowly decreased at an average rate of 0.25 °C/min. While the water vapor concentration was kept stable and as the temperature decreased, the relative humidity at the sample increased. The temperature at which the salt absorbed humidity was determined by the increase in the current signal. The temperature was measured at several locations near the salt to get an accurate reading. A more detailed description of the method can be found in [5].

2.2. Corrosion tests

The corrosion experiments were performed with 20 mm × 20 mm × 5 mm carbon steel (P235GH) coupons. The coupons were first polished in ethanol with 320-grit silicon carbide paper, then with 1000-grit paper, and finally with 2500-grit paper. Then, the coupons were washed in an ultrasound bath in ethanol. Approximately 100 mg of dry NH_4Cl was placed on top of each coupon. The experimental setup is shown in Fig. 3. Four coupons were used in each experiment and were placed on a ceramic sample tray. The temperature was measured at three locations in the sample tray (Fig. 3a), and was within ± 1 °C. The experiments were conducted in a gas atmosphere with 25 vol% water vapor at various temperatures: 71, 72, 80, 105, 120, and 160 °C. The

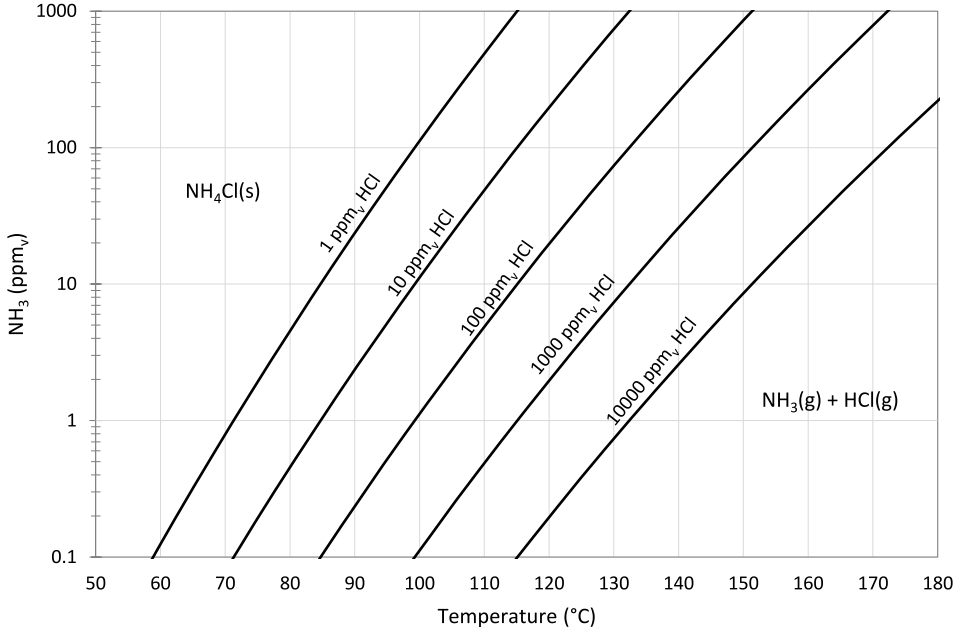

Fig. 1. Thermodynamic stability of NH_4Cl(s) as calculated with FactSage 8.1 [27] using the FactPS database. Note the logarithmic scale on the y-axis.

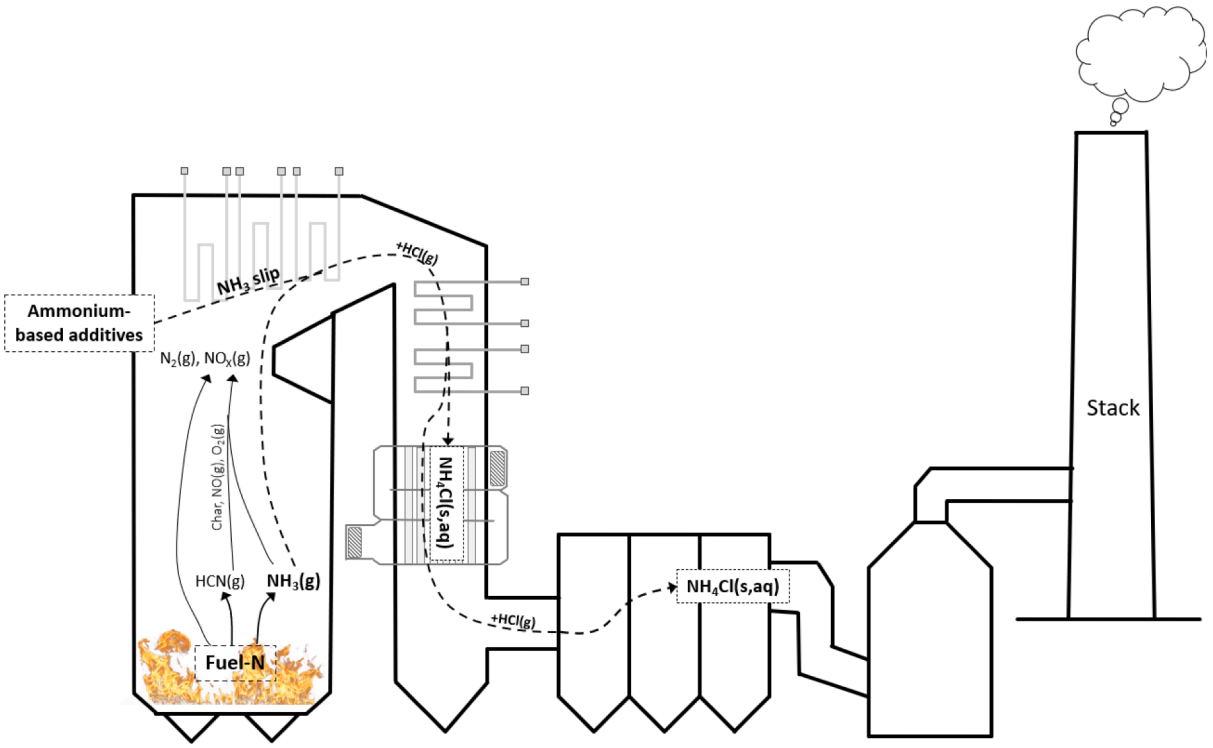

Fig. 2. Formation routes of NH_4Cl from fuel-N, NH_3 slip from additives and HCl(g).

coupons were first heated in a nitrogen atmosphere to the desired temperature. When the temperature was stable, water vapor and oxygen were added to the gas. The total flow was 2 Nl/min, and the O_2 concentration was 5 vol%. The exposure time was 24 h, 48 h, and 168 h. After exposure, one coupon was cast in epoxy, cut, and polished to reveal the cross-section. The metal surface and corrosion products were analyzed using scanning electron microscopy with energy dispersive X-ray spectroscopy (SEM-EDX), LEO Gemini 1530 with a Thermo Scientific UltraDry Silicon Drift Detector (SDD). SEM images of the whole sample cross-section were taken and stitched together to produce a panorama image. The material loss was determined from the panorama images in over 50 000 points by comparing with unexposed samples. Additionally, the mass loss of the coupon was determined by weighing the sample before and after each exposure. After the exposure, the salt

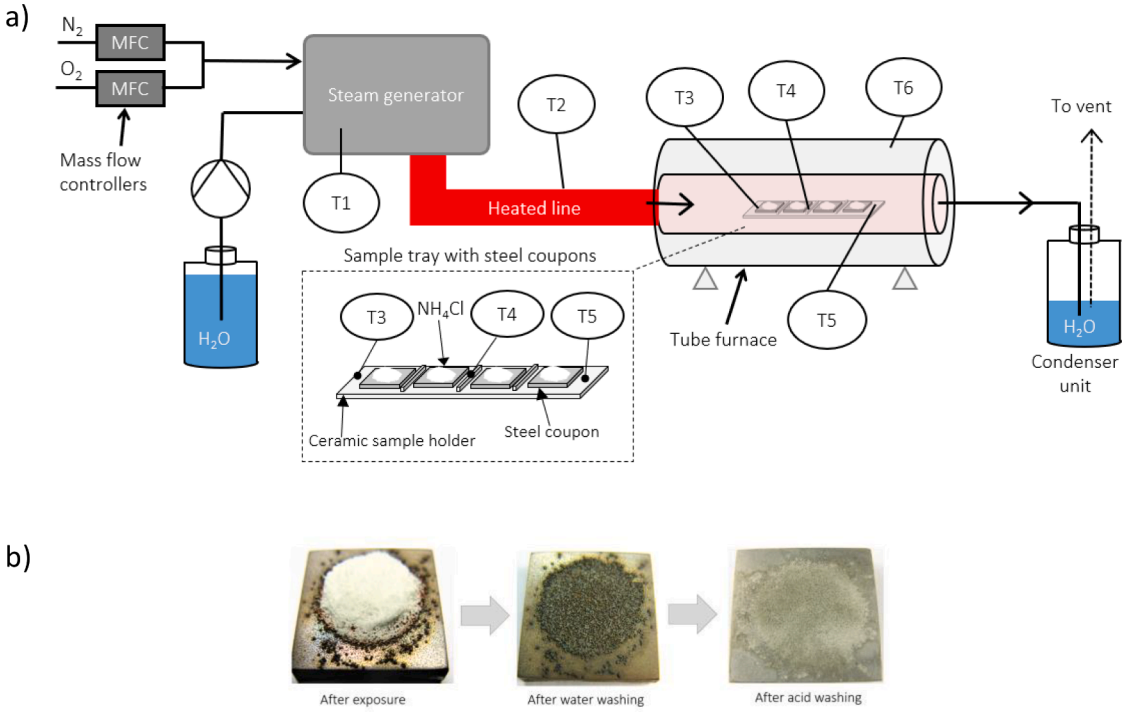

Fig. 3. a) Experimental setup in the corrosion experiments. T1-T6 indicate temperature measurements. b) Example of a sample after exposure to NH_4Cl, 25 vol% H_2O and 5 vol% O_2 for 24 h at 80 °C, and after the washing procedure with water and citric acid.

and corrosion products were removed with a paper towel under water and then dried with acetone before weighing. The remaining corrosion products were removed by citric acid, and the samples were weighed again. The acid step was repeated until all corrosion products were removed and a blank reference sample was used to quantify any metal loss of the sample. Fig. 3b shows and example of a coupon after each washing step. An average corrosion rate was calculated based on the mass loss for the exposed area.

3. Results and discussion

3.1. Hygroscopic properties of NH_4Cl

The current signal from the water uptake measurement by NH_4Cl at 25 vol% is shown in Fig. 4. At the beginning of the test, the current reading was close to zero as the salt was dry. The salt became conductive when the temperature decreased below 92 °C, as seen from the increase in the current signal. This was caused by the water uptake of the salt; however, it is not the deliquescence of the salt, but likely adsorption of water leading to a conductive surface. As the temperature was further lowered, more water uptake occurred and the current signal increased. A second sharp current signal increase was detected at 71 °C, which results from the deliquescence of the salt. This was confirmed in the corrosion measurements of the present study in section 3.2.2, where deliquescence occurred at 71 °C but not at 72 °C after a one-week exposure at 25 vol% H_2O (Fig. 8). As heating of the salt started at 8 h (Fig. 4), the water evaporated and the signal went back to close to zero. Results of measurements with water vapor concentrations between 10 and 35 vol% are shown in Fig. 5. At conditions below the curve, NH_4Cl absorbs some water and can cause corrosion. Deliquescence occurs at a lower temperature; for example, at 25 vol% H_2O, NH_4Cl starts to absorb moisture at about 92 °C while deliquescence occurs at 71 °C. The water dew point is given as a reference in the figure. An empirical equation ($R^2 = 0.99$) for the data presented in Fig. 5 for pH_2O between 0.1 and 0.35 atm was determined:

$$T_{NH_4Cl,\ H_2O\ uptake} = 165.4 \cdot (pH_2O)^{0.4073}$$

where the temperature is in °C and pH_2O is in atm.

Previous corrosion measurements with NH_4Cl on carbon steel and 10 vol% H_2O have shown severe corrosion at 60 °C [11], thus corresponding with the conditions just below the water uptake curve in Fig. 5. The corrosion experiments in this study were performed with 25 vol% H_2O below and above the water uptake curve.

In Fig. 6, the water uptake values are given as relative humidity at the various temperatures. At a higher temperature, NH_4Cl started to absorb moisture at lower relative humidity. It must be pointed out that these values are not DRH values. DRH values for NH_4Cl at these temperatures could not be found in the literature. As discussed earlier, deliquescence at 25 vol% H_2O occurs at 71 °C, which corresponds to a DRH of 78% (±2%). The DRH at 71 °C is close to the values reported for 20–30 °C, where DRH is between 77 and 79% RH [22,28]. Toba et al. [18] reported no corrosion for carbon steel at 20% RH and 80 °C, and at 30–50% RH the corrosion rate was 0.82–1.63 mm/year and increased significantly at 60% RH. The results plotted in Fig. 6 suggest that at 80 °C, NH_4Cl becomes conductive and corrosive at an RH of about 35%.

3.2. Corrosivity of NH_4Cl on carbon steel

3.2.1. 24 h exposure

The mass changes after exposure to 25 vol% H_2O for 24 h at various temperatures are shown in Fig. 7. The photographs of the steel coupons after exposure and after removal of the corrosion products are also shown. At 80 °C, the carbon steel corroded substantially, and the corrosion products were beneath the salt. The experimental conditions at 80 °C and 25 vol% H_2O (RH 54%) are below the water uptake curve in Fig. 5. However, it is clear from the appearance of the salt that deliquescence did not occur at 80 °C. In the corrosion experiment at 105 °C (RH 21%), i.e., just above the water uptake curve in Fig. 5, corrosion did not occur beneath the salt. Instead, some corrosion was detected around the salt and at the edges of the sample. Thus, no corrosion rate could be determined. The discoloration around the salt is most probably attributed to the dissociation of $NH_4Cl(s)$ to $NH_3(g)$ and $HCl(g)$, leading to a corrosive environment. At 160 °C, most of the salt had dissociated, as can be seen in the photograph in Fig. 7. The salt dissociated as no $NH_3(g)$ nor $HCl(g)$ were present in the inlet gas.

3.2.2. One-week exposure

The corrosion rates at 71, 72, and 80 °C, with 25 vol% H_2O and 5 vol % O_2, were further studied with one-week exposures and the results are

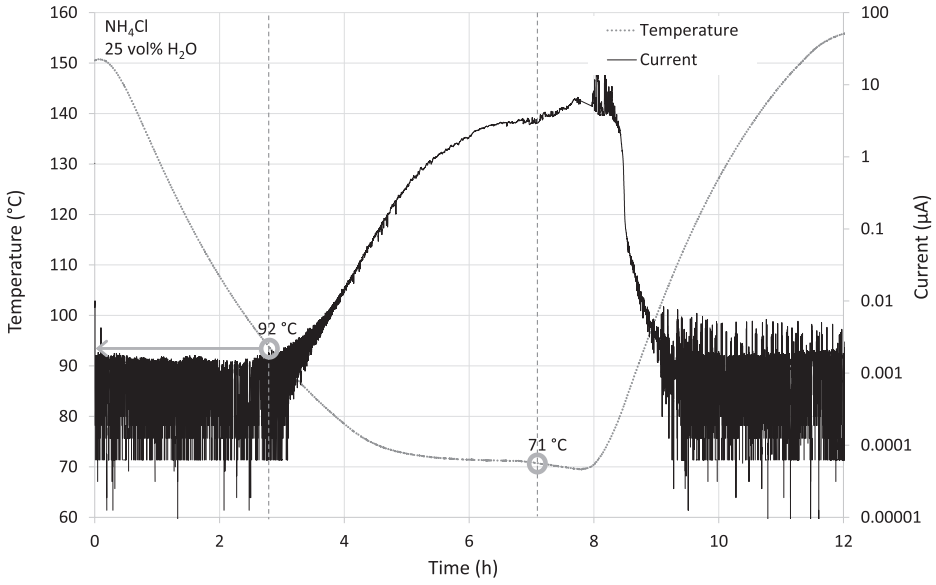

Fig. 4. Temperature and current readings for the determination of water uptake by NH_4Cl at 25 vol% H_2O, using chronoamperometry. Water uptake started at 92 °C and deliquescence at 71 °C.

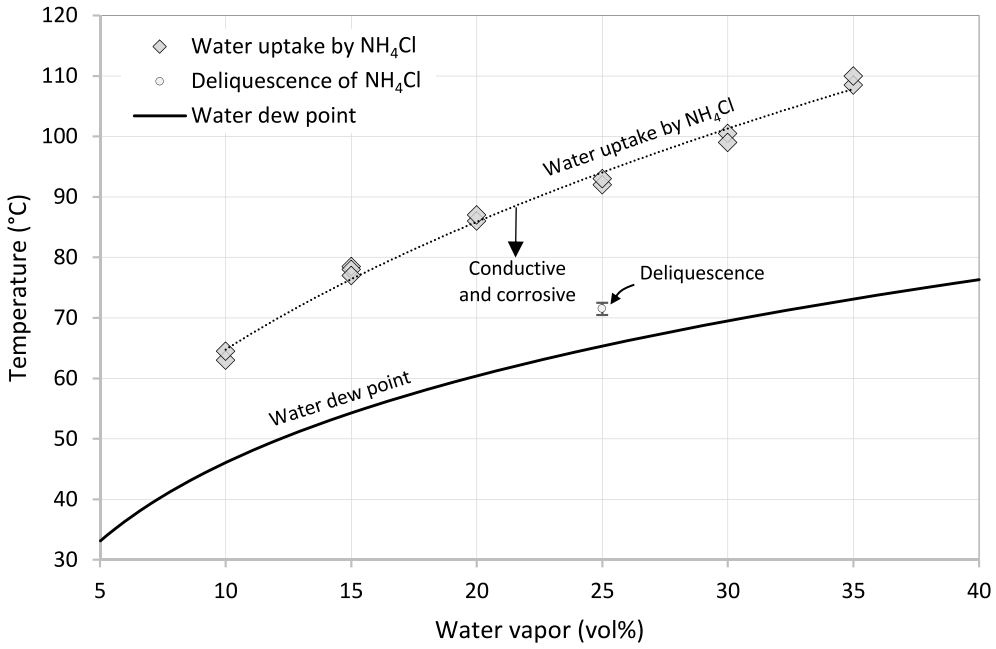

Fig. 5. Water uptake temperatures for NH_4Cl at 10–35 vol% water vapor and deliquescence temperature at 25 vol% water vapor determined with chronoamperometry. At conditions below the water uptake curve, NH_4Cl absorbs water and can cause corrosion.

presented in Fig. 8. Substantial corrosion occurred at 80 °C, and by extrapolating, the results show an average corrosion rate of 4.0 mm/year. The corrosion was much more severe at the lower temperatures, 71 and 72 °C. Interestingly, deliquescence occurred at 71 °C, while at 72 °C the salt had not formed an aqueous solution (photos in Fig. 8). Thus, confirming that the deliquescence temperature for NH_4Cl at 25 vol% H_2O is 71 °C, corresponding to a DRH of 78 ± 2%. Deliquescence did not significantly affect the corrosion compared to the case at 72 °C. The high corrosion rates of around 20 mm/year are in line with a previous study by Sun and Fan [17] of wet corrosion of carbon steel in a concentrated NH_4Cl solution. The corrosiveness of NH_4Cl at relative humidities below the DRH has been studied by Toba et al. [18] in conditions for oil refineries. In their work, NH_4Cl was corrosive when the RH was 30%, and the corrosion rate increased with RH. This was also the case in the present study. The corrosion rate increased with an increase in relative humidity. The relative humidities in the experiments presented in Fig. 8 were: 54% at 80 °C, 75% at 72 °C, and 78% at 71 °C.

Fig. 9 presents the cross-section profiles of the unexposed sample and the samples exposed for 24 h, 48 h, and 168 h. The average and maximum extrapolated corrosion rates determined from SEM panoramas are also given in Fig. 9b-d. Fig. 9a is the profile of an unexposed sample. At the shorter exposures, more variation of the corrosion along the cross-section can be seen. However, after one-week exposure (Fig. 9d), the corrosion was relatively uniform beneath the salt, and the average corrosion of the exposed area was 69 μm. Extrapolating this to a full year gives a corrosion rate of 3.6 mm/year. The maximum corrosion

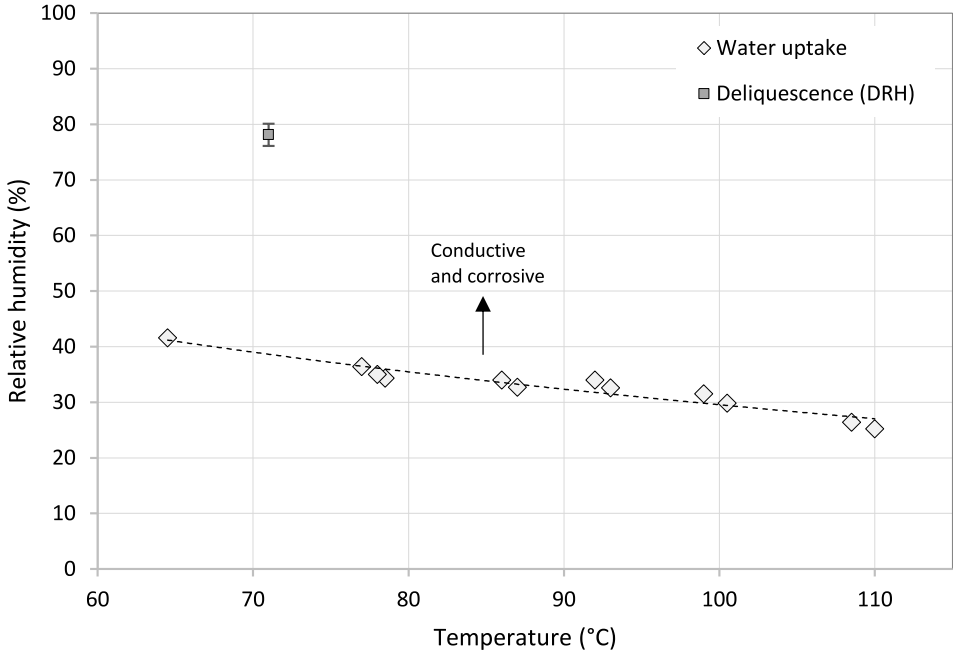

Fig. 6. Relative humidity at which water uptake starts and deliquescence relative humidity (DRH) for NH_4Cl.

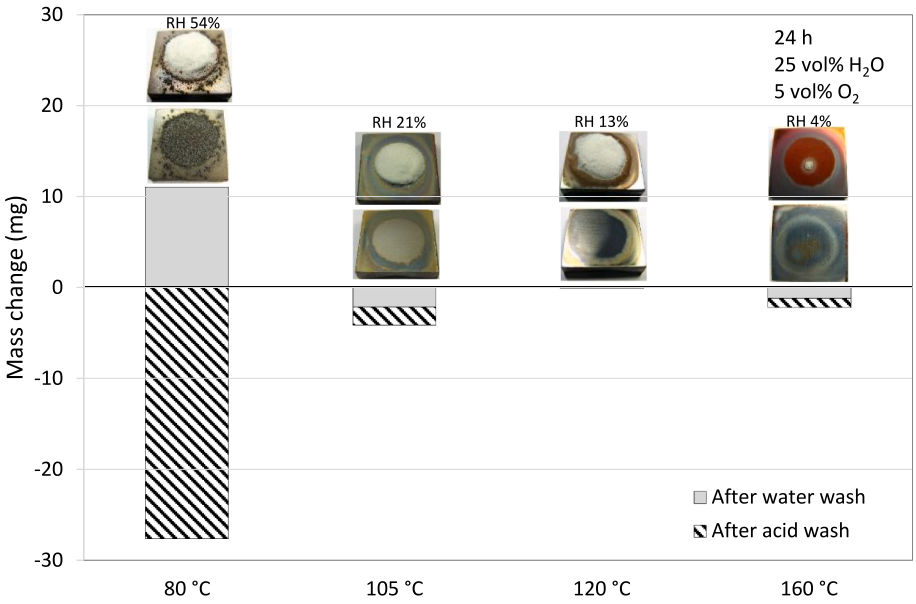

Fig. 7. Mass changes after exposure and after removing the corrosion products with citric acid. Carbon steel (P235GH) was exposed to NH_4Cl at 25 vol%, 5 vol% O_2, 70 vol% N_2 at four temperatures for 24 h. The relative humidities in the experiments are also given.

depth was 99 μm for the one-week exposure (or 5.1 mm/year). The extent of corrosion increased almost linearly from 24 h to 168 h, as can be seen from both the average corrosion determined from the SEM cross-section panorama and mass loss analyses, as shown in Fig. 10.

3.3. Corrosion mechanisms

Fig. 11 presents elemental maps of Fe, O, and Cl from the middle of the carbon steel sample, after exposure to NH_4Cl at 80 °C in 25 vol% H_2O and 5 vol% O_2 for 24, 48, and 168 h, respectively. Interestingly, the chlorine was enriched close to the steel surface with time. Fig. 12a shows an SEM image from the edge of the sample, and Fig. 12b shows selected area analyses. The core of the pit was enriched in chlorine, suggesting the presence of iron chlorides. The area surrounding the core had an oxygen-to-iron atomic ratio of about 3. As iron chlorides come in contact with oxygen and water, iron hydroxides are formed. Then the mobile chlorine ions are transported back to the steel surface. These reactions correspond to an autocatalytic process since HCl is formed in the reaction, lowering the pH and recycling the chlorine.

The main corrosion process and chlorine enrichment near the steel are discussed in detail below. A proposed mechanism for corrosion initiation at RH < DRH is presented in Fig. 13a. Water is adsorbed on the hygroscopic NH_4Cl particle and forms a wetted surface. Capillary condensation in the porous particle or between the steel surface and particle is also possible below the saturation pressure [29]. The unbound water results in the dissociation of NH_4Cl (Reaction (2)), leading to a supersaturated salt solution. Ammonium is a weak acid and will lower the solution's pH (Reaction (3)).

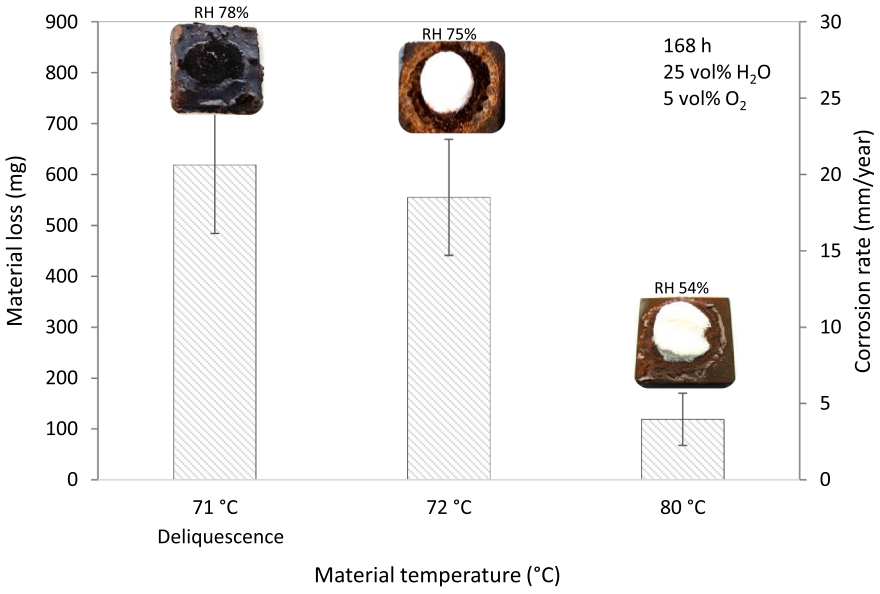

Fig. 8. Material loss and corrosion rate of carbon steel (P235GH) exposed to NH_4Cl at 25 vol%, 5 vol% O_2, 70 vol% N_2 for 168 h. Deliquescence occurred in the experiment at 71 °C. Photographs of the steel coupons after exposure on top. The relative humidities at the three temperatures are also given.

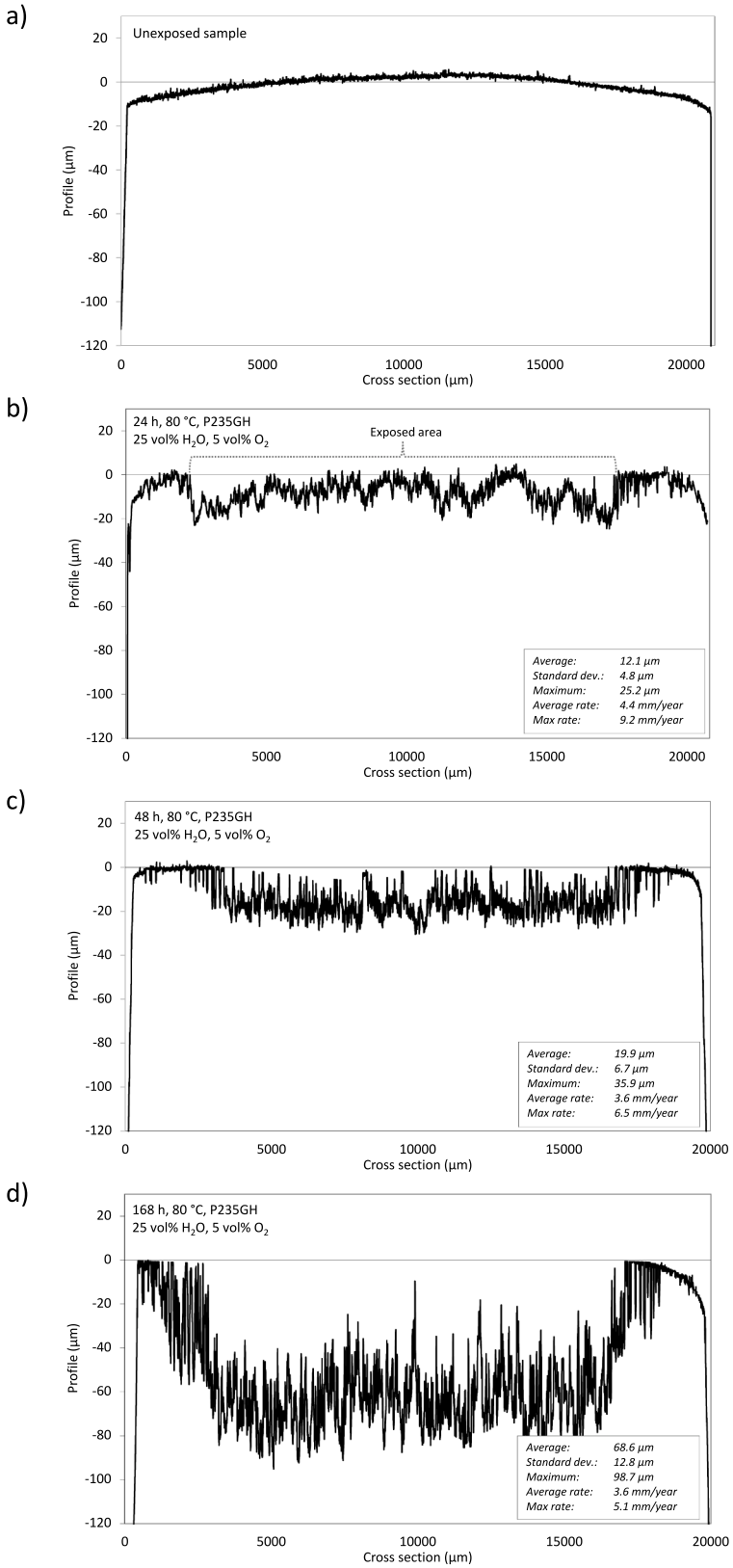

Fig. 9. Sample profiles and material loss as determined from SEM panorama images of the cross section in the middle of the carbon steel samples, for a) an unexposed sample, b) 24 h, c) 48 h, and d) 168 h exposures. b) to c) exposed to NH_4Cl at 80 °C and 25 vol% H_2O, 5 vol% O_2 and rest N_2.

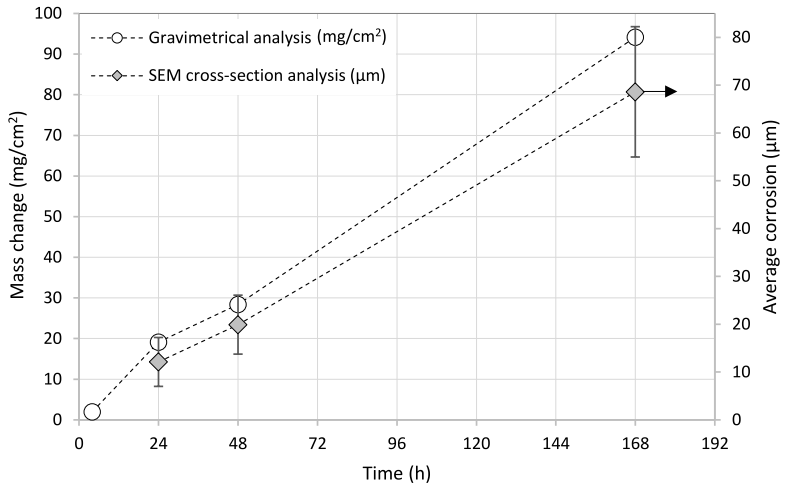

Fig. 10. Material loss as determined from the SEM panoramas and mass loss for carbon steel (P235GH) exposed to NH_4Cl, 25 vol% H_2O, 5 vol% O_2 and rest N_2 at 80 °C.

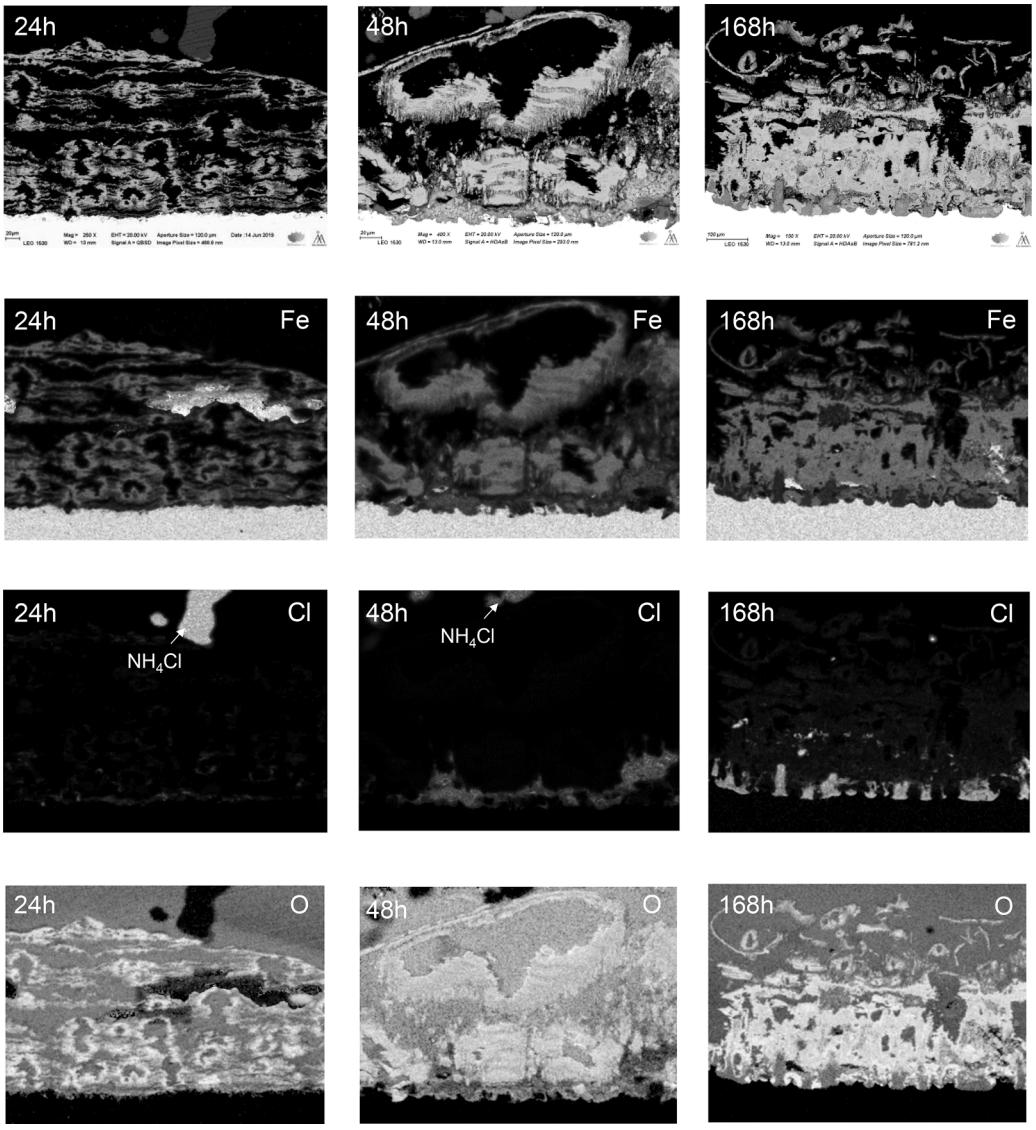

Fig. 11. SEM-EDXA of carbon steel cross-sections' middle part after exposure to NH_4Cl at 80 °C in 25 vol% H_2O, 5 vol% O_2, and 70 vol% N_2 for 24 h, 48 h, and 168 h. SEM images in the top row and X-ray maps of Fe, Cl, and O in the following rows.

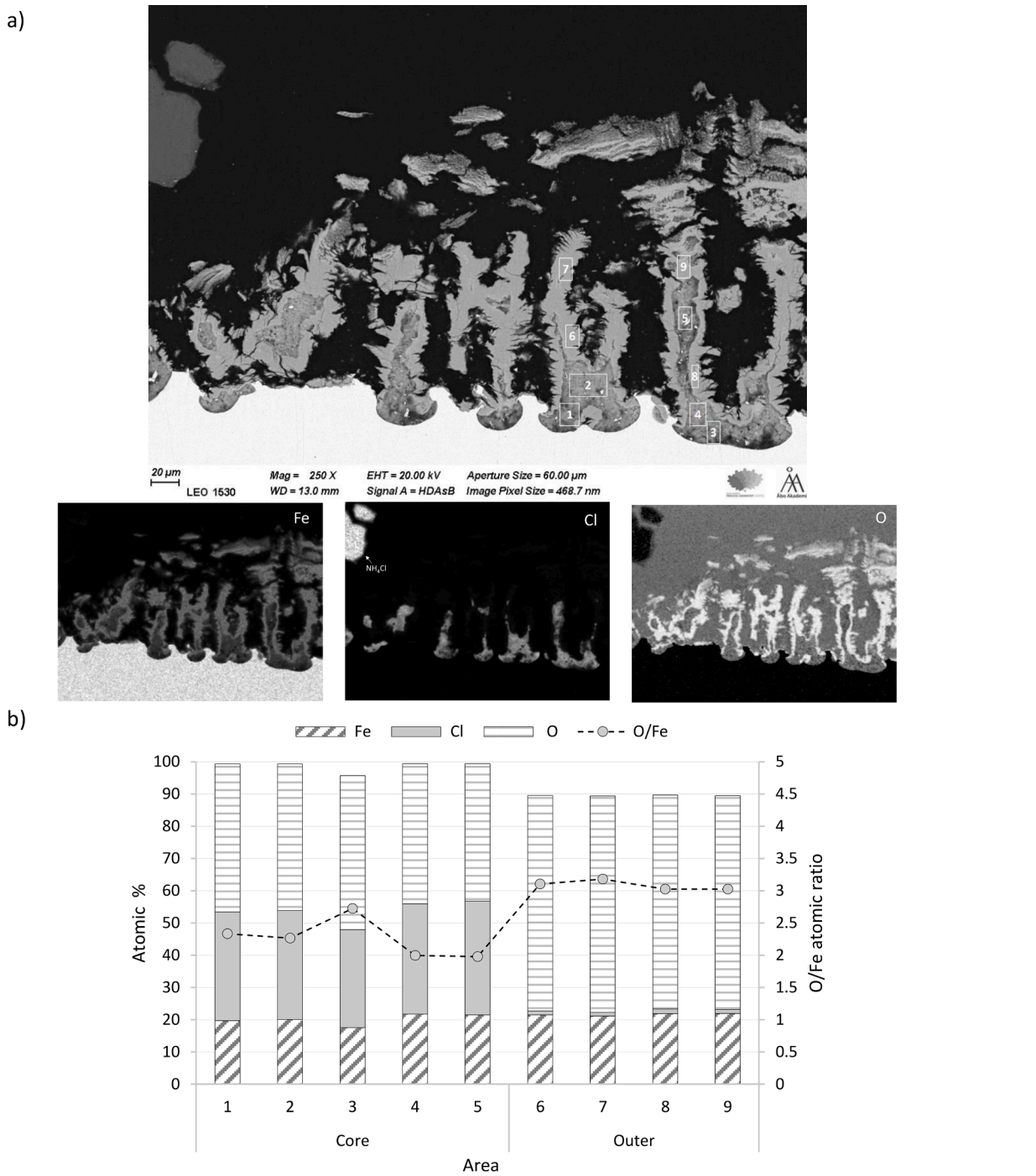

Fig. 12. SEM image and X-ray maps of Fe, Cl, and O in the cross-section of carbon steel sample exposed to NH_4Cl at 80 °C and 25 vol% H_2O, 5 vol% O_2, and rest N_2 for one week. b) Bar chart of Fe, Cl, and O EDX area analyses of the core and outer layer of the corrosion products as marked in the SEM image.

$$NH_4Cl(s) \xrightarrow{H_2O(l)} NH_4^+(aq) + Cl^-(aq) \quad (2)$$

$$NH_4^+(aq) + H_2O(l) \leftrightarrow NH_3(aq) + H_3O^+(aq) \quad (3)$$

These reactions on the steel surface will lead to the oxidation and dissolution of iron according to the anodic reaction (Reaction (4)),

$$Fe(s) \leftrightarrow Fe^{2+}(aq) + 2e^- \quad (4)$$

In acidic conditions, the main cathodic reaction is either hydrogen ion or oxygen reduction (5 and 6):

$$2H^+(aq) + 2e^- \rightarrow H_2(g) \quad (5)$$

$$O_2(g) + 4H^+(aq) + 4e^- \rightarrow 2H_2O(l) \quad (6)$$

Reaction (5) can occur in formed pits where the pH is low. Reaction (6) is limited by the oxygen diffusion to the cathodic site. The oxygen diffusion depends on the ion concentration of the solution, temperature, and corrosion products [30–33].

Fe^{2+} ions close to the steel surface will attract Cl^- ions and form iron chloride (7):

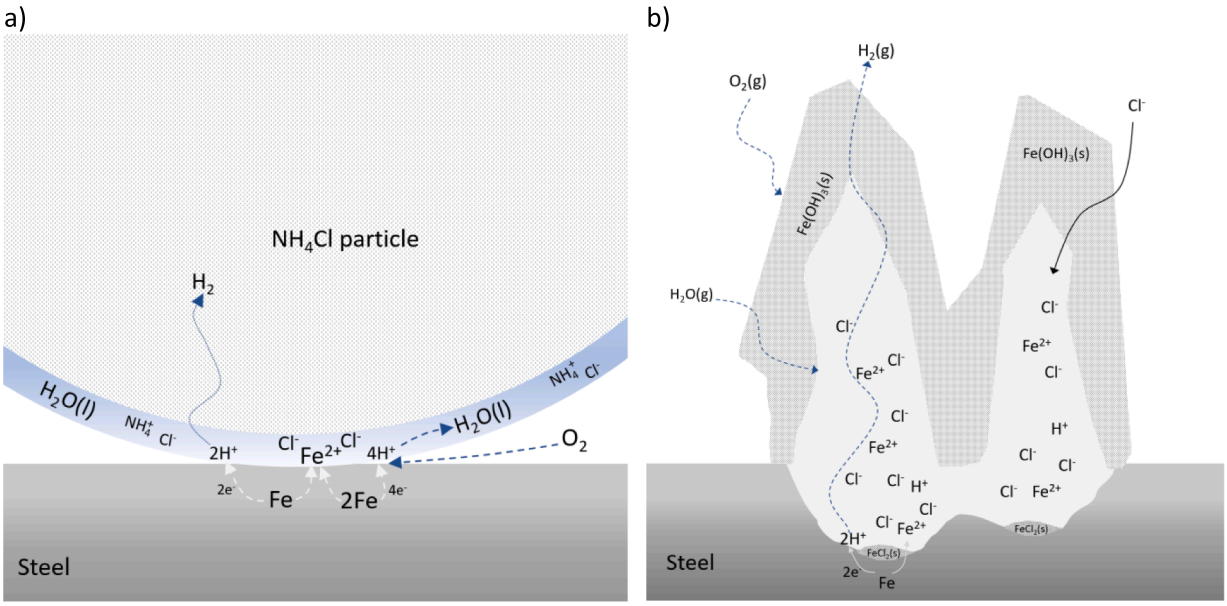

Fig. 13. Proposed corrosion mechanisms of NH_4Cl on carbon steel at RH < DRH. a) Enough water is adsorbed on the NH_4Cl(s) salt particle to wet the surface, initiating the corrosion. b) Iron chloride formation and corrosion evolution.

$$Fe^{2+}(aq) + 2Cl^{-}(aq) \rightarrow FeCl_2(aq,s) \quad (7)$$

Iron chloride may be present as a solid precipitate close to the steel surface [34]. Iron chloride tetrahydrate ($FeCl_2{\cdot}4H_2O$) is highly hygroscopic, and DRH has been reported to be 55% RH at room temperature [35]. In the presence of dissolved oxygen, ferrous (II) hydroxide oxidizes further to ferric (III) hydroxide (Reactions (8) and (9)) [36], forming hematite with time (Reaction (10)):

$$FeCl_2(aq,s) + 2H_2O(l) \rightarrow Fe(OH)_2(s) + 2H^{+}(aq) + 2Cl^{-}(aq) \quad (8)$$

$$4Fe(OH)_2(s) + O_2(g) + 2H_2O(l) \rightarrow 4Fe(OH)_3(s) \quad (9)$$

$$2Fe(OH)_3(s) \rightarrow Fe_2O_3(s) + 3H_2O(g,l) \quad (10)$$

Chloride ions released in Reaction (8) recombine with Fe^{2+} at the steel surface. Chloride ions from the wetted NH_4Cl salt can also diffuse through the corrosion layer, thus leading to a chloride enrichment at the steel surface (Fig. 13b). The formed iron chloride is hygroscopic and possibly leads to an increased corrosion rate.

4. Summary and conclusions

Ammonium chloride, NH_4Cl, can form in the cold-end of boilers in the presence of NH_3(g) and HCl(g). This work explored the hygroscopic properties of NH_4Cl. The conditions at which water uptake starts and the salt is corrosive were determined. Furthermore, corrosion studies with carbon steel at various temperatures were performed at 25 vol% H_2O and 5 vol% O_2. The following conclusions were made:

- The temperature for water uptake by NH_4Cl and wetting of the salt depended on the water vapor concentration. An empirical equation for this was determined for water vapor concentrations between 10 and 35 vol% H_2O.
- The relative humidity at which water uptake started decreased with temperature.
- Deliquescence of NH_4Cl at 25 vol% H_2O occurred at 71 °C. This corresponds to a DRH of 78 ± 2% (at 71 °C).
- Upon water uptake, ammonium chloride was highly corrosive on carbon steel. Corrosion corresponding to several mm/year occurred at 80 °C and 25 vol% H_2O (RH 54%), i.e., at conditions with some water uptake.
- When water was adsorbed, the corrosion rate increased with decreasing temperature and was extremely rapid just above and below the DRH.
- Chlorine was enriched with time on the steel surface due to the formation of hygroscopic iron chloride.
- Mild corrosion of carbon steel observed at higher temperatures was likely due to the dissociation products of NH_4Cl (NH_3(g) and HCl(g)).

The results suggest that severe corrosion of carbon steel by NH_4Cl can be avoided if the material temperatures are maintained above the water uptake temperature for NH_4Cl (approximately 90–120 °C depending on the flue gas water vapor concentration). The formation of NH_4Cl may also be avoided by controlling the NH_3(g) slip and HCl(g) in the flue gas. The presence of NH_3(g) slip and HCl(g) should be verified through measurements at a position where NH_4Cl has not yet formed, i.e., at flue gas temperatures of approximately 100–140 °C, depending on the NH_3(g) and HCl(g) concentrations.

CRediT authorship contribution statement

Emil Vainio: Conceptualization, Methodology, Investigation, Visualization, Writing – original draft, Funding acquisition. **Patrik Yrjas:** Writing – review & editing. **Leena Hupa:** Writing – review & editing. **Mikko Hupa:** Writing – review & editing, Conceptualization.

Declaration of Competing Interest

The authors declare that they have no known competing financial interests or personal relationships that could have appeared to influence the work reported in this paper.

Data availability

Data will be made available on request.

Acknowledgements

This work was financed by the Academy of Finland project

(Properties and behavior of deliquescent salts and deposits in biomass and waste thermal conversion - Towards improved efficiency and reliability, Decision No. 333917). In addition, the support from the CLUE^2-project partners ANDRITZ Oy, Valmet Technologies Oy, UPM-Kymmene Oyj, Metsä Fibre Oy, and International Paper Inc., is gratefully acknowledged. We also want to thank Linus Silvander for carrying out the SEM/EDX analyses, as well as Jaana Paananen and Topias Mannisto for helping with experimental work.

References

[1] Retschitzegger S, Brunner T, Obernberger I. Low-temperature corrosion in biomass boilers fired with chemically untreated wood chips and bark. Energy Fuels 2015;29(6):3913–21.
[2] Brunner T, Reisenhofer E, Obernberger I, Kanziani W, Forstinger M, Vallant R. Low-Temperature Corrosion in Biomass-Fired Combustion Plants - Online Measurement of Corrosion Rates, Acid Dew Points and Deliquescence Corrosion, 25th European Biomass Conference and Exhibition 2017.
[3] Herzog T, Müller W, Spiegel W, Brell J, Molitor D, Schneider D, Corrosion caused by dewpoint and deliquescent salts in the boiler and flue gas cleaning VGL: KG Thome-Kozmiensky og M. Beckmann: Energie aus Abfall Band 9 Neuruppin: TK Verlag 2012; 429–460.
[4] Lindau L, Goldschimdt B. Low temperature corrosion in bark fueled, small boilers. Värmeforsk Services AB 2008:M9–835.
[5] Vainio E, DeMartini N, Hupa L, Åmand L-E, Richards T, Hupa M. Hygroscopic properties of calcium chloride and its role on cold-end corrosion in biomass combustion. Energy Fuels 2019;33(11):11913–22.
[6] Vainio E, Kinnunen H, Laurén T, et al. Low-temperature corrosion in co-combustion of biomass and solid recovered fuels. Fuel 2016;184:957–65.
[7] Vainio E, Laurén T, DeMartini N, Brink A, Hupa M. Understanding low-temperature corrosion in recovery boilers: risk of sulphuric acid dew point corrosion? J-FOR 2014;4(6):14–22.
[8] Ruifeng D, Wenlong W, Fengtao W, Haojun C, Xiajie G. Reason analysis and countermeasures of ammonium chloride crystallization in the flue system of coal-fired power plants after ultra-lowemission transformation. Thermal Power Gener 2018;47(03):128–34.
[9] Bakker W. High temperature corrosion in gasifiers. Mater Res 2004;7(1):53–9.
[10] Jones F, Ryde D, Hjörnhede A. Down-time corrosion in boilers. Fuel Process Technol 2016;141:276–84.
[11] Vainio E, Vänskä K, Laurén T, Yrjas P, Coda Zabetta E, Hupa M, Hupa L. Impact of boiler load and limestone addition on SO_3 and corrosive cold-end deposits in a coal-fired CFB boiler. Fuel 2021;304:121313.
[12] Lindström V. Investigation and risk assessment of low temperature corrosion in a combined heat and power plant, Umeå University, (2016) urn:nbn:se:umu:diva-121629.
[13] Ma L, Wei W, Sun F, Shi Y. Research on formation mechanism of typical low-temperature fouling layers in biomass-fired boilers. Case Stud Thermal Eng 2022;35:102076.
[14] Niu Y, Liu Y, Tan H, Xiong Y, Tongmo X. Origination and formation of NH_4Cl in biomass-fired furnace. Fuel Process Technol 2013;106:262–6.
[15] Akpanyung KV, Loto RT, Fajobi MA. An Overview of Ammonium Chloride (NH_4Cl) Corrosion in the Refining Unit. J. Phys.: Conf. 2019 Ser. 1378 022089.
[16] Liu X, Duan A, Quan J, Jin H, Wang C. A study on the corrosion failure induced by the ammonium chloride deposition in a high-pressure air cooler system. Eng Fail Anal 2020;112:104529.
[17] Sun A, Fan D. Prediction, monitoring, and control of ammonium chloride corrosion in refining processes. CORROSION 2010;6:4649–65.
[18] Toba K, Suzuki T, Kawano K, Sakai J. Effect of Relative Humidity on Ammonium Chloride Corrosion in Refineries, CORROSION 2011;67(5):055005-1–7.
[19] Wexler AS, Seinfeld JH. Second-generation inorganic aerosol model. Atmos Environ A Gen Top 1991;25(12):2731–48.
[20] Kim YP, Seinfeld JH, Saxena P. Atmospheric gas aerosol equilibrium I. Thermodynamic model. Aerosol Sci Technol 1993;19(2):157–81.
[21] Hu D, Chen J, Ye X, Li L, Yang X. Hygroscopicity and evaporation of ammonium chloride and ammonium nitrate: relative humidity and size effects on the growth factor. Atmos Environ 2011;45(14):2349–55.
[22] Adams JR, Merz AR. Hygroscopicity of fertilizer materials and mixtures. lnd Eng Chem 1929;21:305–10.
[23] Qu Q, Li L, Bai W, Yan C, Cao C. Effects of NaCl and NH_4Cl on the initial atmospheric corrosion of zinc. Corros Sci 2005;47(11):2832–40.
[24] Ponkala MJV, Humidity Effects on Hygroscopic Particles Deposited on HEPA Filters and Silicon Wafer Surfaces, Master of Science in Engineering, The University of Texas at Austin December 2012.
[25] Schindelholz E, Risteen BE, Kelly RG. Effect of relative humidity on corrosion of steel under sea salt aerosol proxies I. NaCl. J Electrochem Soc 2014;161(10):C450–9.
[26] Zhu RS, Wang JH, Lin MC. Sublimation of ammonium salts: a mechanism revealed by a first-principles study of the NH_4Cl system. J Phys Chem C 2007;111:13831–8.
[27] Bale CW, Belisle E, Chartrand P, Decterov SA, Eriksson G, Gheribi AE, Hack K, Jung IH, Kang YB, Melançon J, Pelton AD, Petersen S, Robelin C, Sangster J, Spencer P, Van Ende M-A. FactSage Thermochemical Software and Databases - 2010 - 2016. CALPHAD 2016;54:35–53.
[28] Greenspan L. Humidity fixed points of binary saturated aqueous solutions. J Res Natl Bureau of Standards – Phys Chem 1977;81A(1):89–96.
[29] Yarom M, Marmur A. Capillary condensation with a grain of salt. Langmuir 2017;33:13444–50.
[30] Millero FJ, Huang F. Solubility of oxygen in aqueous solutions of KCl, K_2SO_4, and $CaCl_2$ as a function of concentration and temperature. J Chem Eng Data 2003;48:1050–4.
[31] Wang H-b, Li Y, Cheng G-x, Wu W, Zhang Y-h, Li X-y. Electrochemical Investigation of Corrosion of Mild Steel in NH_4Cl Solution. Int J Electrochem Sci 2018;13:5268–83.
[32] Iwai Y, Eya H, ltoh Y, Aral Y, Takeuchi, K. Measurement and Correlation of Solubilities of Oxygen in Aqueous Solutions Containing Salts and Sucrose. Fluid Phase Equilib. 1993; 83: 271−278.
[33] Borgmann CW. Initial corrosion rate of mild steel influence of the cation. Ind Eng Chem 1937;29(7):814–21.
[34] Wranglén G. Pitting and sulphide inclusions in steel. Corros Sci 1974;14:331–4.
[35] Turgoose S. Post-excavation changes in iron antiquities. Stud Conserv 1982;27(3):97–101.
[36] Yamashita M, Konishi H, Kozakura T, Mizuki J, Uchida H. In situ observation of initial rust formation process on carbon steel under Na_2SO_4 and NaCl solution films with wet/dry cycles using synchrotron radiation X-rays. Corros Sci 2005;47:2492–8.